AMERICAN SOCIETY FOR MICROBIOLOGY | mSphere®

RESEARCH ARTICLE
Molecular Biology and Physiology

Glucan Unmasking Identifies Regulators of Temperature-Induced Translatome Reprogramming in *C. neoformans*

Amanda L. M. Bloom,[a] David Goich,[a] Corey M. Knowles,[a] John C. Panepinto[a]

[a]Department of Microbiology and Immunology, Witebsky Center for Microbial Pathogenesis and Immunology, Jacobs School of Medicine and Biomedical Sciences, University at Buffalo, SUNY, Buffalo, New York, USA

ABSTRACT The cell walls of fungi are critical for cellular structure and rigidity but also serve as a major communicator to alert the cell to the changing environment. In response to stresses encountered in human hosts, pathogenic fungi remodel their cell walls. Masking the β-1,3-glucan component of the cell wall is critical to escape detection by innate immune cells. We previously demonstrated that β-1,3-glucan is unmasked in response to host temperature stress when translatome reprogramming is defective in *Cryptococcus neoformans*. Here, we used β-1,3-glucan unmasking as an output to identify signaling modules involved both in masking and in translatome reprogramming in response to host temperature stress. We reveal that the high-osmolarity glycerol (HOG) mitogen-activated protein kinase (MAPK) pathway is involved in translatome reprogramming and that mutants in this pathway display moderate unmasking when grown at 37°C. Additionally, we show that mutants of the cell wall integrity (CWI)/Mpk1 MAPK pathway extensively unmask β-1,3-glucan. While the CWI pathway does not impact translatome reprogramming, our data suggest that it may play a role in the posttranslational regulation of transcription factors that govern masking.

IMPORTANCE *Cryptococcus neoformans* is a fungal pathogen that causes devastating morbidity and mortality in immunocompromised individuals. It possesses several virulence factors that aid in its evasion from the host immune system, including a large polysaccharide capsule that cloaks the antigenic cell wall. Studies investigating how the cell wall is remodeled to keep this pathogen disguised in response to stress have been limited. We previously found that host temperature stress results in translatome reprogramming that is necessary for keeping the highly antigenic β-(1, 3)-glucan component masked. Our data reveal signaling modules that trigger these responses and suggest the points of regulation at which these pathways act in achieving masking. Understanding these mechanisms may allow for therapeutic manipulation that may promote the immune recognition and clearance of this fungal pathogen.

KEYWORDS *Cryptococcus neoformans*, cell signaling, cell wall, glucans, host evasion, stress response

Cryptococcus neoformans is an environmental basidiomycete fungus that is able to enter the mammalian lung and persist. In cases of defective adaptive immunity, it can cause pulmonary infection or disseminate to the central nervous system, where is causes a deadly meningitis. The primary comorbidity associated with cryptococcosis is HIV coinfection; however, recent use of anti-tumor necrosis factor alpha (TNF-α) monoclonal antibodies in the context of rheumatoid arthritis is associated with an increased risk of cryptococcosis (1).

C. neoformans possesses multiple complex traits that promote its persistence in the lung and its virulence. One of these traits, thermotolerance, is required for mammalian

Citation Bloom ALM, Goich D, Knowles CM, Panepinto JC. 2021. Glucan unmasking identifies regulators of temperature-induced translatome reprogramming in *C. neoformans*. mSphere 6:e01281-20. https://doi.org/10.1128/mSphere.01281-20.

Editor Aaron P. Mitchell, University of Georgia

Address correspondence to John C. Panepinto, jcp25@buffalo.edu.

Received 15 December 2020
Accepted 7 January 2021
Published 10 February 2021

infection. Previous work in our laboratory has implicated deadenylation-dependent mRNA decay mediated by Ccr4 in promoting adaptation to host temperature (2–4). This work suggests that reprogramming of the mRNAs associated with translating ribosomes, the translatome, is a prerequisite for temperature adaptation (3). Coupled to temperature adaptation is the maintenance of cell wall integrity (CWI) and the masking of the ubiquitous fungal pathogen-associated molecular pattern (PAMP) β-1,3-glucan.

Another environmental *Cryptococcus* species, *C. amylolentus*, is deficient in thermotolerance and, like our *ccr4*Δ mutant, also unmasks β-1,3-glucan at 37°C (3). In addition, *C. amylolentus* fails to repress abundant ribosomal protein (RP) transcripts, which is necessary for reprogramming the translatome in response to temperature stress. This led us to a model in which thermotolerance and β-1,3-glucan masking are linked, likely via changes that ensue from translatome reprogramming.

We have previously coined the term "adaptive agility," defined as the extent and speed at which an organism can reshape its proteome to one that is suited for its new environment, and speculated that it is essential for and determines an organism's pathogenic potential (5). Host temperature-induced mRNA decay and translatome reprogramming occur immediately in response to stress (3). Posttranslational modifications of proteins allow for rapid, efficient, and dynamic responses by altering the functions of proteins that are already present (6, 7). There have been several examples of how the translational landscape of fungi is regulated by kinases in response to different stressors (5).

The β-1,3-glucan component of the fungal cell wall is highly antigenic. The pattern recognition receptor Dectin-1 specifically recognizes β-1,3-glucan and promotes phagocytosis and inflammatory responses (8). In response to several stressors encountered in the human host, *Candida albicans* engages specific pathways that reduce the exposure of this PAMP. The CEK1-mediated mitogen-activated protein kinase (MAPK) pathway seems to generally regulate β-1,3-glucan masking (9), and signaling through the protein kinase A pathway is required for β-1,3-glucan masking in hypoxic and iron-limiting conditions (10, 11). Interestingly, the Gpr1 receptor, but not the canonical downstream cyclic AMP (cAMP) pathway, regulates lactate-induced masking in *C. albicans* (12). While the cell wall integrity MAPK pathway has been identified in *C. neoformans* (13), pathways that regulate glucan masking specifically in response to stressors have not been investigated.

In this report, we investigate the linkage between glucan masking, translatome reprogramming, and thermotolerance by using β-1,3-glucan unmasking as the phenotypic output of a screen of kinase deletion mutants. We identify two core MAP kinase modules that mediate glucan masking. Mechanistic investigation of the point of action suggests that the Hog1 pathway regulates unmasking via translatome reprogramming, whereas the cell integrity pathway likely regulates unmasking posttranslationally, perhaps through the activation of transcription factors.

RESULTS

A screen of kinase mutants for glucan unmasking implicates core MAP kinases. Reprogramming of the *C. neoformans* translatome through the action of the mRNA deadenylase Ccr4 is required for both temperature adaptation and the maintenance of masking of β-1,3-glucan at the host temperature (3). We reasoned that identification of regulators of glucan masking might also identify factors that control translatome reprogramming in *C. neoformans*. Using β-1,3-glucan unmasking as an output, we screened mutants from the *C. neoformans* kinase deletion collection that were predicted to be sensitive to either the host temperature or cell wall stress (14) and identified two core mitogen-activated protein kinase (MAPK) modules that unmask β-1,3-glucan at 37°C, as detected by flow cytometry. Null mutants for the three components of the Hog1 MAPK pathway, namely, MAP3K *pbs2*Δ, MAP2K *ssk2*Δ, and MAPK *hog1*Δ, exhibit a moderate level of unmasking, defined as 2- to 5-fold over that of the wild type (WT). In addition, all three components of the cell integrity MAPK signaling

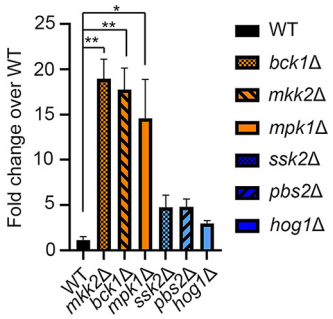

FIG 1 Validation of β-(1,3)-glucan unmasking in kinase mutants of the CWI MAPK and HOG1 MAPK pathways. Kinase mutants grown overnight in YPD at 37°C were stained with anti-β-(1,3)-glucan antibody and assessed for fluorescence by flow cytometry. Fluorescent populations of mutants were compared to the WT to calculate fold change in β-(1,3)-glucan exposure. Statistical analysis was performed with the Kruskal-Wallis test. Error bars depict standard errors of the means (SEM) ($n = 3$ or 4). *, $P < 0.05$; **, $P < 0.01$.

pathway were found to unmask extensively, defined as unmasking at a level greater than 5-fold over the wild-type level. This is true for MAP3K *bck1*Δ, MAP2K, *mkk2*Δ, and MAPK *mpk1*Δ. We went on to validate the screen in larger-scale cultures and found that the identified mutants did indeed reproducibly unmask at 37°C (Fig. 1). Comparison of glucan exposure by fluorescence microscopy to that of the WT, which completely masks β-glucan, and the *ccr4*Δ mutant, which exposes β-glucan, confirmed our findings by flow cytometry and revealed extensive unmasking in a speckled pattern around the periphery of a large portion of the cell wall integrity MAPK mutants and moderate unmasking in a crescent-like pattern around the periphery of a subpopulation of the Hog1 MAPK pathway mutants when grown at 37°C (Fig. 2).

Unmasking kinase mutants exhibit differential sensitivity to temperature and cell wall perturbation. Given that the identified kinase mutants exhibit unmasking at mammalian host temperature, we tested sensitivity to both host temperature stress and cell wall stressors by spot dilution assays (Fig. 3A). All of the mutants demon-

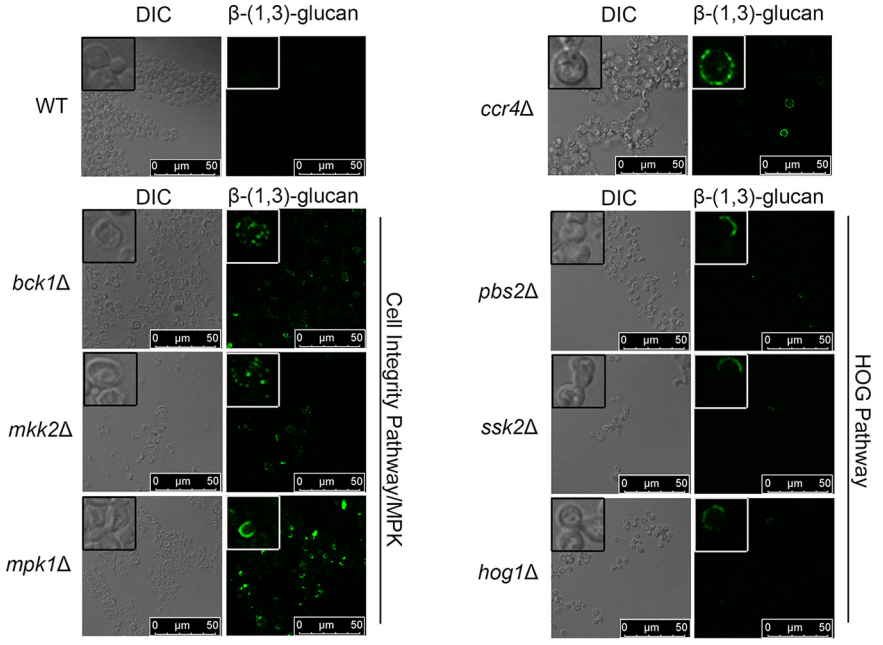

FIG 2 Mutant strains null for components in the CWI MAPK and HOG MAPK pathways unmask β-(1,3)-glucan at 37°C. Cells grown overnight at 37°C were stained with an anti-β-(1,3)-glucan antibody and imaged by fluorescence microscopy. Insets show a portion of the larger image at ×4 magnification. DIC, differential inference contrast.

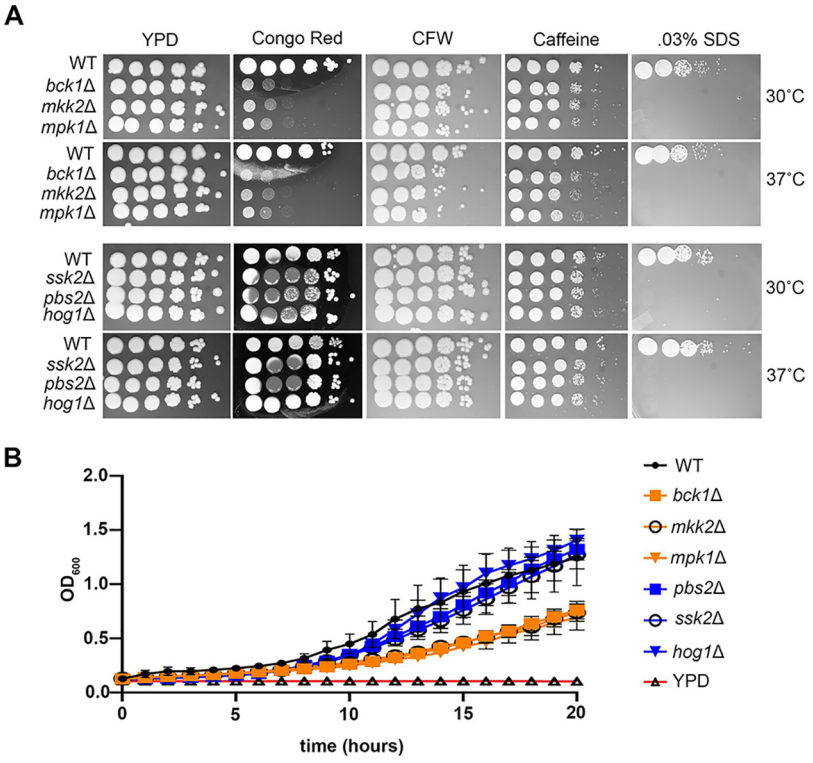

FIG 3 Mutant strains null for components in the CWI MAPK and HOG MAPK pathways display differential sensitivities to cell wall and host temperature stress. (A) Overnight cultures were diluted to an OD_{600} of 1.0, serially diluted 10-fold, spotted onto YPD agar plates containing the indicated compounds, and incubated at 30°C or 37°C. (B) Mid-logarithmic-phase cultures grown at 30°C were diluted to an OD_{600} of 0.1 and grown in a 96-well plate at 37°C. OD_{600}s were recorded over 20 h.

strated a strong sensitivity to SDS and moderate sensitivity to caffeine. All of the cell integrity MAPK pathway mutants exhibited pronounced sensitivity to Congo red, a dye that interacts with β-1,3-glucans, and a modest sensitivity to calcofluor white. None of the mutants exhibited growth defects when they were spotted onto yeast extract-peptone-dextrose (YPD) agar plates and incubated at 37°C, nor were the cell wall stress sensitivities exacerbated at elevated temperatures.

To further examine the effect of host temperature, we also determined growth curves for the mutants in liquid YPD media at 37°C. We have observed differences in growth between liquid and solid media, and it has recently been shown that humidity plays a role in viability and transmission (15). While the Hog1 MAPK mutants demonstrated WT-like growth, all of the CWI MAPK mutants demonstrated slower growth in liquid media despite exhibiting comparable growth by the spot dilution method (Fig. 3B).

Hog1, but not Mpk1, controls unmasking at the level of translatome reprogramming. Our previous data demonstrate that deadenylation-dependent mRNA decay promotes the reprogramming of the translatome to allow for expression of genes required for temperature adaptation and glucan masking. We next set out to investigate if Hog1 and Mpk1 act at the level of translatome reprogramming. The first step in translatome reprogramming is the rapid, but transient, removal of highly abundant and efficiently translated mRNAs from the translating pool (16). In the wild type, nearly every ribosomal protein mRNA is removed from the translating pool by 1 h at 37°C (3). Removal of ribosomal protein mRNAs permits the association of transcription factor mRNAs and stress response effector mRNAs with ribosomes. We asked if transient repression of *RPL2*, a representative ribosomal protein mRNA, was intact in the identified unmasking mutants of each pathway. Analysis of *RPL2* repression by Northern blotting revealed a decreased rate of repression in the *pbs2*Δ, *ssk2*Δ, and

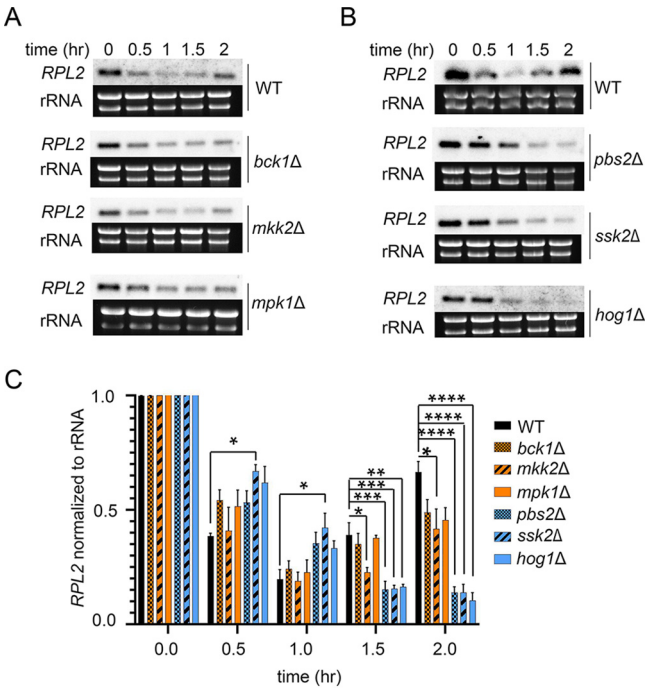

FIG 4 Only Hog1 upstream regulators work at the level of translatome reprogramming. (A) Mid-logarithmic-phase cultures were shifted to 37°C for 2 h. *RPL2* levels, normalized to rRNA levels, were quantified by Northern blotting analysis. Gels and blots are representative of 3 biological replicates. (B) The graph depicts mean *RPL2* levels following a shift to 37°C. Statistical analysis was performed using one-way ANOVA with Dunnett's *post hoc* test, by comparing normalized levels of expression of *RPL2* in the mutants to its expression level in the WT. Error bars represent SEM ($n = 3$). *, $P < 0.05$; **, $P < 0.01$, ***, $P < 0.001$; ****, $P < 0.0001$.

*hog1*Δ mutants compared to that in the wild type (Fig. 4). *RPL2* repression in the *bck1*Δ, *ssk2*Δ, and *mpk1*Δ mutants exhibited the same repression kinetics as the wild type, with a rapid decline in levels during the first hour, followed by a gradual increase toward prestress levels. These data suggest that the Hog1 pathway, but not the Mpk1 cell integrity pathway, regulate the first step in translatome reprogramming.

Temperature adaptation in *C. neoformans* is accompanied by a moderate translational repression consistent with the removal of a large group of highly abundant and highly translated mRNAs from the translating pool. We reasoned that if RP transcripts were delayed in their removal from the translating pools in the *hog1*Δ mutant, then we might observe a defect in host temperature-associated changes in the translational landscape. We used polysome profiling to compare the translational states of the wild type, the *mpk1*Δ mutant, and the *hog1*Δ mutant at 30 min after a shift to 37°C (Fig. 5). Like the WT, the *mpk1*Δ mutant exhibited a decrease in the number of low-molecular-weight polysomes and an increase in the number of high-molecular-weight polysomes in response to host temperature. The *hog1*Δ mutant demonstrated a defect in translational regulation, with very little change in the polysomes and a large increase the 60S subunit. This is consistent with the Hog1 pathway regulating glucan masking through translatome reprogramming.

Hog1 and Mpk1 are activated during host temperature adaptation. We next sought to establish that these phenotypes in the *hog1*Δ and *mpk1*Δ mutants are due to direct participation of these kinase modules during host temperature adaptation. In order to evaluate this, we measured the levels of active phosphorylated Hog1 and Mpk1 by Western blotting in WT cells during growth at 37°C (Fig. 6, left). We found that shifting to 37°C activated both kinases in the WT, with pronounced activation occurring after 1 h.

The observed delay in RP transcript decay in the *hog1*Δ mutant suggested that

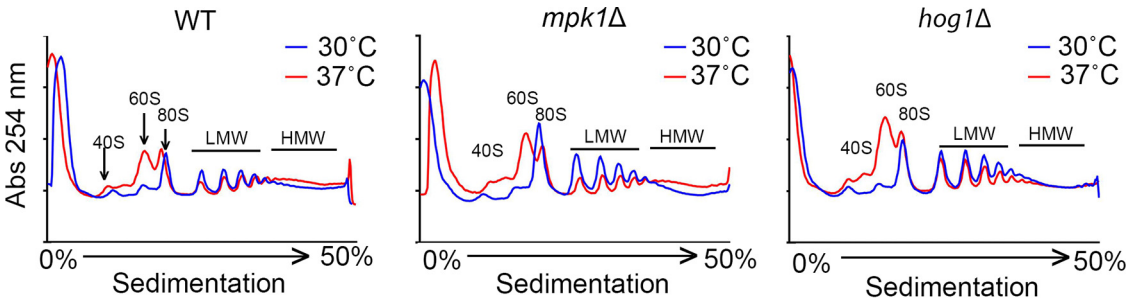

FIG 5 Hog1, but not Mpk1, impacts host temperature-induced changes in the translational landscape. Each strain was grown to mid-log phase in YPD at 30°C. Cells were collected from 30°C cultures and cultures that were shifted to 37°C for 30 min. Polysome profiles were obtained from reading the absorbance at 254 nm of lysates that were separated in sucrose gradients by ultracentrifugation. Profiles are representative of 3 biological replicates. The 40S, 60S, and 80S (monosome) peaks are labeled (with arrows in the WT profile). Low- and high-molecular-weight (LMW and HMW, respectively) polysomes are indicated. In response to host temperature, LMW polysomes are slightly reduced, with a concomitant increase in HMW polysomes and 60S subunit peaks in the WT.

Hog1 activity influences removal of RP transcripts from actively translating ribosomes. We wondered then if Hog1 activation would be reduced in the absence of RP transcript decay. To test this, we also examined Hog1 and Mpk1 activation in a *ccr4*Δ mutant, which is severely deficient in RP decay (3) (Fig. 6, right). We found that temperature-induced Hog1 activation was delayed in the *ccr4*Δ mutant, beginning after 2 h, and was not as robust as in the wild type. We also observed a small but reproducible acceleration in Mpk1 activation in the *ccr4*Δ mutant. Together, these results indicate that both the Hog1 and Mpk1 kinase modules participate in adaptation to growth at 37°C and that, while Ccr4-mediated mRNA decay is not a prerequisite for Mpk1 activation, Ccr4 either directly or indirectly modulates Hog1 activation during host temperature adaptation.

Ccr4, Hog1, and Mpk1 cooperatively regulate the host temperature transcriptome. In the absence of deadenylation-dependent mRNA decay, many transcription factors fail to enter the translatome, leading to gross defects in transcriptome reprogramming (3). In order to evaluate potential genes involved in the glucan-masking phenotype, we compared the existing *mpk1*Δ transcriptome sequencing (RNA-seq) data set (17; GEO accession no. GSE57217) to our own data set from the *ccr4*Δ mutant (3; accession no. GSE121183) (Fig. 7A). We filtered the resulting overlap of 232 genes for those that would be cell surface associated or involved in cell wall remodeling, and among these genes were two chitin synthases, *CHS4* and *CHS5*, as well as an uncharacterized exoglucanase, *EXG1*, which were predicted to be downregulated in both sets. We hypothesized that if Hog1 influences removal of RP mRNAs and, thus, translatome reprogramming and if translatome reprogramming precedes transcriptome remodeling as we predict (Fig. 8), then these genes would also be affected in the *hog1*Δ mutant. We reported previously that *CHS6* was downregulated in the *ccr4*Δ mutant and included that in our analysis. We compared the levels of expression of these four genes by reverse transcription-quanti-

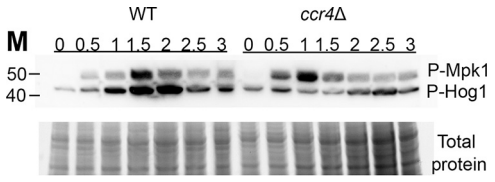

FIG 6 Activation of Hog1 and Mpk1 during growth at mammalian body temperature. WT and *ccr4*Δ cells were grown to mid-log phase in YPD at 30°C and then shifted to 37°C for 3 h, and aliquots were pelleted for protein extraction every half hour. Lysates were probed by Western blotting for phosphorylation of Hog1 and Mpk1 (P-Mpk1 and P-Hog1, respectively) using a cross-reactive antibody. Total protein is shown as a loading control. Data shown are representative of three biological replicates.

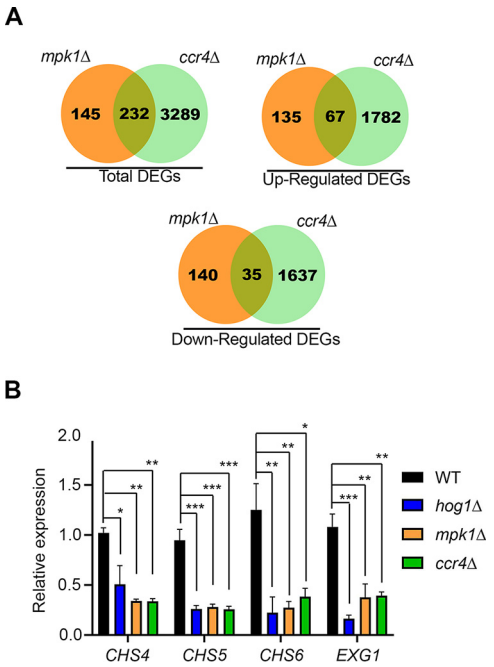

FIG 7 Genes involved in cell wall remodeling are downregulated in unmasking mutants at 37°C. (A) Differentially expressed genes (DEGs) in the *mpk1*Δ and *ccr4*Δ strains were compared to identify genes regulated by both the CWI pathway and Ccr4-mediated mRNA decay. (B) The WT, *hog1*Δ, *mpk1*Δ, and *ccr4*Δ strains were grown to mid-log phase in YPD at 30°C and then shifted to 37°C for 1 h. qPCR was performed on cDNA from these cells to evaluate the expression of *CHS4*, *CHS5*, *CHS6*, and *EXG1*. The $\Delta\Delta C_T$ method was used to calculate expression normalized to that of mitofusin. Statistical analysis was performed using one-way ANOVA with Dunnett's *post hoc* test by comparing the normalized expression of each gene in the mutants to their expression in the WT. Error bars depict SEM ($n = 3$). *, $P < 0.05$; **, $P < 0.01$; ***, $P < 0.001$.

tative PCR (RT-qPCR) in the WT and the *mpk1*Δ, *ccr4*Δ, and *hog1*Δ mutants, following a shift to 37°C for 1 h (Fig. 7B). We observed a statistically significant downregulation of all four cell wall genes in each of the mutant strains. This finding indicates that Hog1, Mpk1, and Ccr4 all coordinate the expression of cell wall genes at 37°C and suggests that these proteins cooperatively enforce the transcriptional regulon involved in glucan masking.

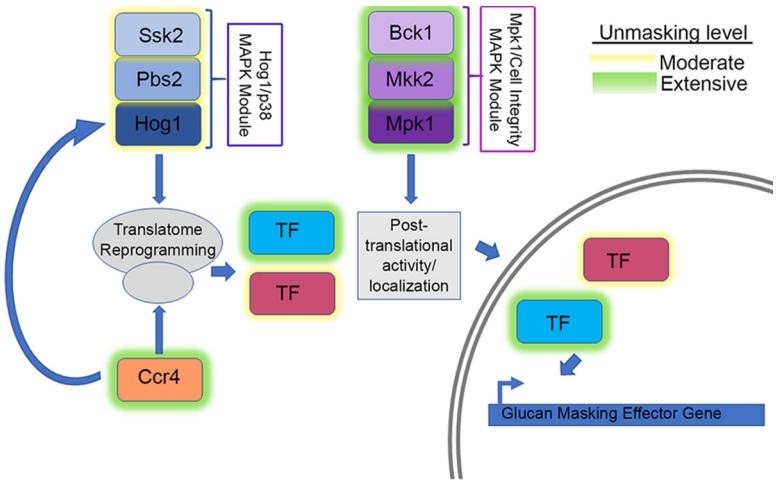

FIG 8 Model for the role of the CWI MPK and HOG MPK pathways in host temperature-induced β-(1,3)-glucan unmasking. Our data suggest that the HOG MAPK pathway acts at the level of translatome reprogramming. The decay of RP transcripts may impact the activation of Hog1, perhaps via a complex feedback loop. The CWI MAPK pathway does not affect translatome reprogramming but may act downstream on newly synthesized transcription factors (TF) that govern glucan masking.

DISCUSSION

The fungal cell wall is essential and not only impacts the structure and rigidity of the cell but also mediates all interactions that the cell encounters with its environment. It is logical then that this structure is dynamic and displays plasticity. β-1,3-Glucan is an important component of fungal cell walls, serving to anchor other components by covalent attachment (18). It is also highly antigenic in the context of a host, and exposure of this glucan results in rapid detection by Dectin-1, resulting in protective immune responses (19). Pathogenic fungi utilize mechanisms of glucan masking to help evade the host immune system. While *C. albicans* hides its glucan layer under a blanket of mannoproteins (20), *Aspergillus* species mask β-1,3-glucan with the hydrophobic surface protein RodA on conidia (21) and a polysaccharide cloak of galactosaminogalactan on hyphae (22), and *C. neoformans* is protected by a polysaccharide capsule (23). The continual changes that a pathogen encounters in a host must elicit responses that include cell wall remodeling to keep it cloaked from attack.

Unlike in other pathogenic fungi, β-1,3-glucan is not the most abundant cell wall carbohydrate in *C. neoformans*; however, it is essential, as deletion of the sole β-1,3-glucan synthase, *FKS1*, is lethal (24, 25). Studies investigating β-1,3-glucan masking have been lacking for this organism. We previously reported that Ccr4-mediated mRNA decay and translatome reprogramming in response to host temperature was required for keeping β-1,3-glucan masked. Here, we identified additional signaling modules that mediate this outcome.

The Pkc1 CWI MAPK pathway is the major pathway that regulates cell wall integrity in *C. neoformans* (13); thus, we were not surprised to find that mutants with mutations in this pathway unmasked β-1,3-glucan. Like the Cek1 MAPK pathway in *C. albicans* (9), this pathway may control masking in a general manner by regulating genes that are involved in cell wall structure even under no stress, as these mutants are inherently sensitive to cell wall stressors. In fact, mutation of the most upstream kinase of this pathway, Pck1, is viable only in the presence of an osmostabilant (26). Host temperature may increase reliance on this pathway to help in combating stress-induced insult to the cell wall. The terminal kinase Mpk1 was previously reported to be activated in response to oxidative and nitrosative stresses (26); we show here that it is activated in response to 37°C and may explain both the growth defect in liquid culture at 37°C and the extensive β-(1, 3)-glucan unmasking seen in strains with null mutations in the kinase components of this pathway (Fig. 1 and 3B). We showed that Mpk1 activation in response to temperature stress was not hindered when translatome reprogramming was inhibited by defective clearance of ribosomes in the *ccr4*Δ mutant (Fig. 6). Further, RP transcript repression (Fig. 4) and polysome profiles (Fig. 5) were unaffected in the *mpk1*Δ mutant, suggesting that the CWI MAPK pathway does not impact unmasking at the level of translatome reprogramming. Given that our previous data suggest that translatome reprogramming impacts transcription factor production and precedes transcriptional remodeling, we speculate that CWI MPK regulation of masking in response to host temperature acts in parallel with or after translatome reprogramming, perhaps through posttranslational modification of newly translated transcription factors, thereby affecting their activity or localization (Fig. 8). Indeed, our previous work identified several genes that encode transcription factors that are downregulated in the *ccr4*Δ mutant that may be influenced by Mpk1, which was supported by the overlap of differentially expressed genes in these two strains (Fig. 6A). Importantly, we note that the RNA-seq data for the *mpk1*Δ strain was acquired from cells grown in YPD supplemented with the osmostabilant sorbitol due to the original inclusion of the *pck1*Δ mutant in those studies (17), while our data were acquired from cells that were stressed at mammalian host temperature for 1 h in YPD. Differential gene expression may be even greater in the *mpk1*Δ mutant in medium that does not aid in stabilizing the cell membrane. Regardless, the data suggest that Ccr4-mediated changes in gene expression in response to host temperature include components involved in regulation

of the CWI MAPK pathway or targets of the CWI-MAPK pathway that promote glucan masking.

The *C. neoformans* HOG MPK pathway has been studied largely in regard to osmoregulation and drug resistance (27–29). Interestingly, Hog1 negatively regulates capsule production, and in response to osmotic stress, the constitutive activation of Hog1 in *C. neoformans* is downregulated (27, 28). We show here that Hog1 activation is heightened in response to host temperature, and this activation is dependent, at least in part, on Ccr4-mediated clearance of actively translating ribosomes (Fig. 6). Intriguingly, the absence of *HOG1* resulted in significantly delayed repression of the abundant RP transcripts following a shift to 37°C. These mRNAs need to be cleared from ribosomes for translatome reprogramming to ensue. Delayed RP repression was supported by the lack of change in the translational landscape in response to host temperature in the *hog1*Δ mutant. If Hog1 activation were a prerequisite for Ccr4-mediated decay, then we would have expected Hog1 phosphorylation to occur in the *ccr4*Δ mutant similarly to in the WT, but this was not the case. The relationship between Hog1 activation and translatome reprogramming is therefore complex, and the following begs to be answered: at which time point in the temperature response does Hog1 act? In *Saccharomyces cerevisiae*, Hog1 has been indirectly linked to translational regulation via activation of its downstream target Rck2, which targets the translation elongation factor eEF2 (30). We are currently investigating the events that occur at the ribosome in response to stress to identify the order of operations that result in translatome reprogramming. Our work suggests that Hog1 is required for the immediate repression of RP transcripts and their exit from the translating pool to allow for translation of newly synthesized genes, such as those involved in masking (Fig. 8). The fact that the *hog1*Δ mutant grows as well as the WT at 37°C suggests that translatome reprogramming eventually occurs; however, glucan masking is not completely achieved. Future assessment of phagocytosis will determine if Hog1-mediated β-(1, 3)-glucan masking contributes to host evasion and if the loss of Hog1-mediated β-(1, 3)-glucan masking alters the immune landscape in the lung.

Our work here is the first to examine signaling modules that specifically play a role in the masking of the antigenic cell wall component β-(1, 3)-glucan in *C. neoformans*. Given that innate immunity is equipped to specifically recognize this pattern-associated molecular pattern and elicit protective immune responses, an understanding of the pathogen's ability to cloak itself may be essential in future therapeutic endeavors, and given that protein translation has proven to be targetable, the role of factors that specifically manipulate the translational machinery to promote pathogen adaptation may be instrumental.

MATERIALS AND METHODS

Strains used in this study. For all experiments, the *C. neoformans* serotype A var. *grubii* strain H99 was used as the WT. Kinase mutants were created by the Y. S. Bahn laboratory (14) and obtained from the fungal genetics stock center. The *ccr4*Δ mutant was created by biolistic transformation of the H99 strain using a PCR-amplified DNA construct in which the nourseothricin resistance cassette was flanked by sequences upstream and downstream of the *CCR4* gene. The URA resistance cassette was dropped from our previously constructed plasmid (31) and replaced with NAT. Primers for cloning and amplification are listed in Table 1. The knockout clone was verified by PCR and Southern and Northern blotting.

β-1,3-Glucan staining and detection. For screening of the kinase mutant library, cells were grown overnight in 100 μl of YPD in a 96-well plate at 37°C. Cells were pelleted, washed twice in phosphate-buffered saline (PBS), and then stained in a 96-well plate according to the staining protocol below. For verification of identified mutants from the screen, cells were grown in 3 ml of YPD overnight at 37°C, with shaking at 250 rpm. Cells were washed once in PBS and resuspended in PBS to an optical density at 600 nm (OD_{600}) of 1.0. For each strain, 100 μl of cells was aliquoted to 2 microcentrifuge tubes and pelleted. For staining, cells were resuspended in 100 μl of PBS containing 15 μg/ml anti-β-(1, 3)-glucan antibody (Biosupplies Australia). For no primary controls, cells were resuspended in 100 μl of PBS. All tubes were incubated at 37°C with gentle rotation for 1 h. Cells were pelleted and washed 3 times with PBS and resuspended in PBS containing 10 μg/ml Alexa Fluor 488-goat anti-mouse secondary antibody. Cells were incubated at 37°C with gentle rotation for 40 min while being protected from light. Cells were pelleted and washed three times in PBS and then fixed in 3.7% formaldehyde at room temperature for 20 min while being protected from light. Finally, cells were washed and resuspended in PBS. For microscopy, cells were visualized and images captured using a Leica SP8 TCS confocal microscope. For

TABLE 1 Oligonucleotide sequences used in this study

Primer	Sequence (5′–3′)
F-CCR4up	AGTGAGACAAGAAGTTGGGC
R-CCR4down	ATCGTGTCCTCTACCTCGC
F-NAT-BglII	TAATAAAGATCTGCTGCGAGGATGTGAGCTGG
R-NAT-MunI	TAATAACAATTGAAGCTTATAGAAGAGATGTAGAAACTAGC
CHS4 F[a]	CGGTCTTCAGGCATTGATTT
CHS4 R[a]	TTCGGAGTGAAGTGATGCTG
CHS5 F[b]	GCTTGGATGATCTTCTATATCTG
CHS5 R[b]	TACCTTCATCATGGATGACA
CHS6 F[a]	TTGACCCTTGGCACATCT
CHS6 R[a]	GTTGGCATAAGTATCCTT
EXG1 F	ACCCAGATGAGTATGACGC
EXG1 R	GCCAGAACCACTACATTGG
mitofusin F	CCTGGATCTTCCTCACCG
mitofusin R	CAGGTGCAACTGAGAGCG

[a]*CHS4* and *CHS6* primers were previously published (32).
[b]Primers for *CHS5* were previously published (33).

flow cytometry, fluorescence was measured using a BD LSRFortessa flow cytometer. Statistical analysis for flow cytometry was done using GraphPad Prism (version 8.4.3).

Growth curves. All strains were grown overnight in 3 ml of YPD at 30°C, with shaking at 250 rpm. Overnight cultures were used to seed fresh YPD cultures to an OD_{600} of 0.15 and were grown at 30°C for 5 h. These mid-logarithmic cultures were then diluted to an OD_{600} of 0.1 in a 100-μl final volume in a 96-well plate. Growth was assessed by measuring the OD_{600} every 10 min for 20 h using a Biotek Synergy hybrid plate reader.

Spot plate analyses. For spot plate analyses, all strains were grown in 3 ml of YPD overnight at 30°C. Cells were washed twice with sterile deionized water (SDW) and resuspended in SDW at an OD_{600} of 1.0. Five 10-fold serial dilutions were prepared in SDW, and 5 μl of each dilution was spotted onto YPD agar plates supplemented with cell wall inhibitors (0.5 mg/ml caffeine, 1 mg/ml calcofluor white, 5 mg/ml Congo red, 0.03% SDS). Plates were incubated at 30°C or 37°C for 3 days and photographed.

Polysome profiling. Polysome profiling was done as previously published (3), with minimal differences. Briefly, cells were grown to mid-log phase in YPD, and half of the culture was pelleted, resuspended in prewarmed 37°C YPD, and incubated at 37°C for 30 min. Cycloheximide (0.1 mg/ml) was added immediately, and cells were pelleted by centrifugation at 4,000 rpm and 4°C for 3 min. Pellets were flash frozen in liquid nitrogen and stored at −80°C until lysis. Pellets were washed in polysome lysis buffer (20 mM Tris HCl, pH 8.0, 140 mM KCl, 5 mM $MgCl_2$, 1% Triton X-100, 25 mg/ml heparin sodium sulfate, 0.1 mg/ml cycloheximide) and pelleted. Cells were resuspended in residual buffer, transferred to a microcentrifuge tube, and pelleted at 13,000 rpm for 30 s. The supernatant was removed, and pellets were resuspended in 100 μl of cold lysis buffer and transferred to an Eppendorf tube containing glass beads. Cells were lysed mechanically in a Bullet Blender for 5 min, followed by the addition of 300 μl cold lysis buffer. The supernatant was transferred to a cold microcentrifuge tube and centrifuged for 5 min at 14,000 rpm and 4°C. Cleared lysates were quantitated for RNA, and 250 μg was loaded on top of 10% to 50% sucrose gradients. Gradients were subjected to ultracentrifugation for 2 h at 39,000 rpm and 4°C. Sucrose gradients were then pushed through a flow cell, and RNA was detected by UV-visible light to determine the A_{254}.

Northern blot assessment of *RPL2* mRNA repression. For all strains, cells were grown in 3 ml of YPD at 30°C and 250 rpm overnight. Overnight cultures were used to seed 40 ml of YPD at an OD_{600} of 0.2. Cells were grown at 30°C, with shaking at 250 rpm, until the OD_{600} reached 0.6. Cells were pelleted and resuspended in prewarmed 37°C YPD. Aliquots of 5 ml were pelleted every 30 min for 2 h and flash frozen in liquid nitrogen. Pellets were resuspended in 50 μl of buffer RLT (Qiagen RNeasy kit) plus 10 μl/ml β-mercaptoethanol (β-ME), and cells were lysed by mechanical disruption with glass beads using a Bullet Blender. Lysates were resuspended in 450 μl of RLT plus β-ME, and RNA was extracted using the Qiagen RNeasy kit. For Northern blot analysis of *RPL2*, 3 μg of RNA per sample was electrophoretically separated in a 1% agarose-formaldehyde gel. The rRNA was detected and quantified by ImageLab software. RNA was transferred to a nylon membrane, hybridized with a P32-labeled *RPL2* DNA probe, and detected by phosphorimaging using a Typhoon scanner. *RPL2* signal was quantified using ImageLab software. *RPL2* levels were normalized to corresponding rRNA. Statistical analysis was performed using GraphPad Prism (version 8.4.3).

Western blot detection of phospho-Hog1 and phospho-Mpk1. The *C. neoformans ccr4*Δ strain and the wild-type parental strain (H99) were used to inoculate 5 ml overnight YPD cultures, shaken at 250 rpm at 30°C. Overnight cultures were used the following day to inoculate fresh YPD (at an OD_{600} of 0.2), followed by 5 h of shaking in baffled flasks in a 30°C incubator until mid-log phase (OD_{600} = 0.65). Mid-log-phase cells were pelleted, resuspended in prewarmed YPD, and shaken in a 37°C incubator at 250 rpm, with images recorded every half hour. At each time point, cells were pelleted, the supernatant was discarded, and the pellets were rapidly frozen in liquid nitrogen and stored at −80° until lysis.

Thawed pellets were rinsed in 1 ml SDW and then resuspended in whole-cell lysis buffer (15 mM HEPES [pH 7.4], 10 mM KCl, 5 mM $MgCl_2$, 10 μl/ml Halt protease inhibitor, 1 mM dithiothreitol [DTT]). Cells were lysed by mechanical disruption using glass beads in a Bullet Blender, and the resulting lysate was clarified by centrifugation. Samples were reduced and denatured by boiling them in Laemmli buffer with β-ME, and 30 μg of protein per sample was electrophoretically separated through a Bio-Rad stain-free Tris-glycine gel. Prior to the transference of protein to nitrocellulose, the gel was imaged and total protein was quantified from the gel using ImageLab software. The blot was probed using a rabbit anti-phospho-p38 MAPK (Cell Signaling Technologies), followed by an anti-rabbit HRP secondary antibody, and visualized by chemiluminescence using a Bio-Rad ChemiDoc Imager. It was found that the phospho-p38 primary antibody, in addition to detecting phosphorylated Hog1, was cross-reactive with phosphorylated Mpk1. The specificity of this cross-reactive band was verified using a mouse anti-phospho-p42/44 MAPK antibody (Cell Signaling Technologies), which demonstrated the loss of the corresponding band in the *mpk1*Δ mutant and reliably showed the same pattern of Mpk1 phosphorylation as the phospho-p38 antibody across all biological replicates. The phospho-p38 signal was selected to show the phosphorylation of both Hog1 and Mpk1 due to its higher signal-to-noise ratio.

RT-qPCR. The *C. neoformans hog1*Δ, *mpk1*Δ, and *ccr4*Δ strains and the wild-type parental strain (H99) were grown in 5-ml overnight cultures in YPD and shaken at 30°C and 250 rpm. Overnight cultures were used the following day to inoculate fresh YPD (OD_{600} = 0.2), followed by 5 h of shaking in baffled flasks in a 30°C incubator until mid-log phase (OD_{600} = 0.65). Mid-log-phase cells were pelleted and resuspended in prewarmed YPD and shaken in a 37°C incubator at 250 rpm for 1 h. Cells were then pelleted, flash frozen in liquid nitrogen, and stored at −80°C until further processing. Pellets were thawed on ice and resuspended in RLT buffer (Qiagen RNeasy kit) with 10 μl/ml β-ME, and cells were lysed by mechanical disruption with glass beads using a Bullet Blender. The crude lysate was clarified by centrifugation, and RNA was extracted from the soluble fraction using the Qiagen RNeasy kit. Genomic DNA was digested using the Qiagen RNeasy kit for on-column DNase I digestion, and equal quantities of eluted RNA were converted to cDNA using the high-capacity cDNA reverse transcription kit with RNase inhibitor (ThermoFisher). qPCR for *CHS4* (CNAG_00546), *CHS5* (CNAG_05818), *CHS6* (CNAG_06487), *EXG1* (CNAG_05803), and mitofusin (CNAG_06688) were performed on cDNA using the qPCR SyGreen Blue mix LoROX (PCR Biosystems) according to the manufacturer's instructions. Primers for each gene can be found in Table 1. The data were acquired on a CFX Connect real-time PCR detection system (Bio-Rad). Mitofusin (CNAG_06688) was used as an internal control, and negative-control samples without reverse transcriptase were included. Two technical replicates and three biological replicates were performed for all reactions. The $\Delta\Delta C_T$ method (where C_T is threshold cycle) was used to calculate differences in expression. Statistical analysis was performed using GraphPad Prism (version 8.2.1), with significance defined as follows: *, $P < 0.05$; **, $P < 0.01$; and ***, $P < 0.001$. One-way analysis of variance (ANOVA) was performed with Dunnett's *post hoc* test comparing the normalized expression of each gene to its expression in wild-type H99.

ACKNOWLEDGMENTS

The kinase deletion collection was obtained from the Fungal Genetics Stock Center (Manhattan, KS, USA).

We declare that the research was conducted in the absence of any commercial or financial relationships that could be construed as a potential conflict of interest.

A.L.M.B., D.G., and J.C.P. conceived and designed the experiments. A.L.M.B., D.G., and C.M.K. performed the experiments. A.L.M.B., D.G., and J.C.P. wrote the manuscript.

This work was funded by grant NIH R01 AI131977 to J.C.P.

REFERENCES

1. Liao T-L, Chen Y-M, Chen D-Y. 2016. Risk factors for cryptococcal infection among patients with rheumatoid arthritis receiving different immunosuppressive medications. Clin Microbiol Infect 22:815.e1–815.e3. https://doi.org/10.1016/j.cmi.2016.05.030.
2. Bloom AL, Solomons JT, Havel VE, Panepinto JC. 2013. Uncoupling of mRNA synthesis and degradation impairs adaptation to host temperature in Cryptococcus neoformans. Mol Microbiol 89:65–83. https://doi.org/10.1111/mmi.12258.
3. Bloom ALM, Jin RM, Leipheimer J, Bard JE, Yergeau D, Wohlfert EA, Panepinto JC. 2019. Thermotolerance in the pathogen Cryptococcus neoformans is linked to antigen masking via mRNA decay-dependent reprogramming. Nat Commun 10:4950. https://doi.org/10.1038/s41467-019-12907-x.
4. Havel VE, Wool NK, Ayad D, Downey KM, Wilson CF, Larsen P, Djordjevic JT, Panepinto JC. 2011. Ccr4 promotes resolution of the endoplasmic reticulum stress response during host temperature adaptation in Cryptococcus neoformans. Eukaryot Cell 10:895–901. https://doi.org/10.1128/EC.00006-11.
5. Leipheimer J, Bloom ALM, Panepinto JC. 2019. Protein kinases at the intersection of translation and virulence. Front Cell Infect Microbiol 9:318. https://doi.org/10.3389/fcimb.2019.00318.
6. Spoel SH. 2018. Orchestrating the proteome with post-translational modifications. J Exp Bot 69:4499–4503. https://doi.org/10.1093/jxb/ery295.
7. Zhang Q, Bhattacharya S, Pi J, Clewell RA, Carmichael PL, Andersen ME. 2015. Adaptive posttranslational control in cellular stress response pathways and its relationship to toxicity testing and safety assessment. Toxicol Sci 147:302–316. https://doi.org/10.1093/toxsci/kfv130.
8. Brown GD, Herre J, Williams DL, Willment JA, Marshall AS, Gordon S. 2003. Dectin-1 mediates the biological effects of beta-glucans. J Exp Med 197:1119–1124. https://doi.org/10.1084/jem.20021890.
9. Galan-Diez M, Arana DM, Serrano-Gomez D, Kremer L, Casasnovas JM, Ortega M, Cuesta-Dominguez A, Corbi AL, Pla J, Fernandez-Ruiz E. 2010. Candida albicans beta-glucan exposure is controlled by the fungal CEK1-mediated mitogen-activated protein kinase pathway that modulates immune responses triggered through dectin-1. Infect Immun 78:1426–1436. https://doi.org/10.1128/IAI.00989-09.

10. Pradhan A, Avelar GM, Bain JM, Childers D, Pelletier C, Larcombe DE, Shekhova E, Netea MG, Brown GD, Erwig L, Gow NAR, Brown AJP. 2019. Non-canonical signalling mediates changes in fungal cell wall PAMPs that drive immune evasion. Nat Commun 10:5315. https://doi.org/10.1038/s41467-019-13298-9.
11. Pradhan A, Avelar GM, Bain JM, Childers DS, Larcombe DE, Netea MG, Shekhova E, Munro CA, Brown GD, Erwig LP, Gow NAR, Brown AJP. 2018. Hypoxia promotes immune evasion by triggering beta-glucan masking on the Candida albicans cell surface via mitochondrial and cAMP-protein kinase A signaling. mBio 9:e01318-18. https://doi.org/10.1128/mBio.01318-18.
12. Ballou ER, Avelar GM, Childers DS, Mackie J, Bain JM, Wagener J, Kastora SL, Panea MD, Hardison SE, Walker LA, Erwig LP, Munro CA, Gow NA, Brown GD, MacCallum DM, Brown AJ. 2016. Lactate signalling regulates fungal beta-glucan masking and immune evasion. Nat Microbiol 2:16238. https://doi.org/10.1038/nmicrobiol.2016.238.
13. Gerik KJ, Donlin MJ, Soto CE, Banks AM, Banks IR, Maligie MA, Selitrennikoff CP, Lodge JK. 2005. Cell wall integrity is dependent on the PKC1 signal transduction pathway in Cryptococcus neoformans. Mol Microbiol 58:393–408. https://doi.org/10.1111/j.1365-2958.2005.04843.x.
14. Lee KT, So YS, Yang DH, Jung KW, Choi J, Lee DG, Kwon H, Jang J, Wang LL, Cha S, Meyers GL, Jeong E, Jin JH, Lee Y, Hong J, Bang S, Ji JH, Park G, Byun HJ, Park SW, Park YM, Adedoyin G, Kim T, Averette AF, Choi JS, Heitman J, Cheong E, Lee YH, Bahn YS. 2016. Systematic functional analysis of kinases in the fungal pathogen Cryptococcus neoformans. Nat Commun 7:12766. https://doi.org/10.1038/ncomms12766.
15. Springer DJ, Saini D, Byrnes EJ, Heitman J, Frothingham R. 2013. Development of an aerosol model of Cryptococcus reveals humidity as an important factor affecting the viability of Cryptococcus during aerosolization. PLoS One 8:e69804. https://doi.org/10.1371/journal.pone.0069804.
16. Bloom AL, Panepinto JC. 2014. RNA biology and the adaptation of Cryptococcus neoformans to host temperature and stress. Wiley Interdiscip Rev RNA 5:393–406. https://doi.org/10.1002/wrna.1219.
17. Donlin MJ, Upadhya R, Gerik KJ, Lam W, VanArendonk LG, Specht CA, Sharma NK, Lodge JK. 2014. Cross talk between the cell wall integrity and cyclic AMP/protein kinase A pathways in Cryptococcus neoformans. mBio 5:e01573-14. https://doi.org/10.1128/mBio.01573-14.
18. Garcia-Rubio R, de Oliveira HC, Rivera J, Trevijano-Contador N. 2019. The fungal cell wall: Candida, Cryptococcus, and Aspergillus species. Front Microbiol 10:2993. https://doi.org/10.3389/fmicb.2019.02993.
19. Taylor PR, Tsoni SV, Willment JA, Dennehy KM, Rosas M, Findon H, Haynes K, Steele C, Botto M, Gordon S, Brown GD. 2007. Dectin-1 is required for beta-glucan recognition and control of fungal infection. Nat Immunol 8:31–38. https://doi.org/10.1038/ni1408.
20. Gantner BN, Simmons RM, Underhill DM. 2005. Dectin-1 mediates macrophage recognition of Candida albicans yeast but not filaments. EMBO J 24:1277–1286. https://doi.org/10.1038/sj.emboj.7600594.
21. Carrion S. d J, Leal SM, Ghannoum MA, Aimanianda V, Latgé J-P, Pearlman E. 2013. The RodA hydrophobin on Aspergillus fumigatus spores masks dectin-1- and dectin-2-dependent responses and enhances fungal survival in vivo. J Immunol 191:2581–2588. https://doi.org/10.4049/jimmunol.1300748.
22. Gravelat FN, Beauvais A, Liu H, Lee MJ, Snarr BD, Chen D, Xu W, Kravtsov I, Hoareau CM, Vanier G, Urb M, Campoli P, Al Abdallah Q, Lehoux M, Chabot JC, Ouimet MC, Baptista SD, Fritz JH, Nierman WC, Latge JP, Mitchell AP, Filler SG, Fontaine T, Sheppard DC. 2013. Aspergillus galactosaminogalactan mediates adherence to host constituents and conceals hyphal beta-glucan from the immune system. PLoS Pathog 9:e1003575. https://doi.org/10.1371/journal.ppat.1003575.
23. O'Meara TR, Alspaugh JA. 2012. The Cryptococcus neoformans capsule: a sword and a shield. Clin Microbiol Rev 25:387–408. https://doi.org/10.1128/CMR.00001-12.
24. Gilbert NM, Donlin MJ, Gerik KJ, Specht CA, Djordjevic JT, Wilson CF, Sorrell TC, Lodge JK. 2010. KRE genes are required for beta-1,6-glucan synthesis, maintenance of capsule architecture and cell wall protein anchoring in Cryptococcus neoformans. Mol Microbiol 76:517–534. https://doi.org/10.1111/j.1365-2958.2010.07119.x.
25. Thompson JR, Douglas CM, Li W, Jue CK, Pramanik B, Yuan X, Rude TH, Toffaletti DL, Perfect JR, Kurtz M. 1999. A glucan synthase FKS1 homolog in cryptococcus neoformans is single copy and encodes an essential function. J Bacteriol 181:444–453. https://doi.org/10.1128/JB.181.2.444-453.1999.
26. Gerik KJ, Bhimireddy SR, Ryerse JS, Specht CA, Lodge JK. 2008. PKC1 is essential for protection against both oxidative and nitrosative stresses, cell integrity, and normal manifestation of virulence factors in the pathogenic fungus Cryptococcus neoformans. Eukaryot Cell 7:1685–1698. https://doi.org/10.1128/EC.00146-08.
27. Bahn YS, Kojima K, Cox GM, Heitman J. 2005. Specialization of the HOG pathway and its impact on differentiation and virulence of Cryptococcus neoformans. Mol Biol Cell 16:2285–2300. https://doi.org/10.1091/mbc.e04-11-0987.
28. Ko YJ, Yu YM, Kim GB, Lee GW, Maeng PJ, Kim S, Floyd A, Heitman J, Bahn YS. 2009. Remodeling of global transcription patterns of Cryptococcus neoformans genes mediated by the stress-activated HOG signaling pathways. Eukaryot Cell 8:1197–1217. https://doi.org/10.1128/EC.00120-09.
29. Kim SY, Ko YJ, Jung KW, Strain A, Nielsen K, Bahn YS. 2011. Hrk1 plays both Hog1-dependent and -independent roles in controlling stress response and antifungal drug resistance in Cryptococcus neoformans. PLoS One 6:e18769. https://doi.org/10.1371/journal.pone.0018769.
30. Teige M, Scheikl E, Reiser V, Ruis H, Ammerer G. 2001. Rck2, a member of the calmodulin-protein kinase family, links protein synthesis to high osmolarity MAP kinase signaling in budding yeast. Proc Natl Acad Sci U S A 98:5625–5630. https://doi.org/10.1073/pnas.091610798.
31. Panepinto JC, Komperda KW, Hacham M, Shin S, Liu X, Williamson PR. 2007. Binding of serum mannan binding lectin to a cell integrity-defective Cryptococcus neoformans ccr4Delta mutant. Infect Immun 75:4769–4779. https://doi.org/10.1128/IAI.00536-07.
32. Esher SK, Ost KS, Kohlbrenner MA, Pianalto KM, Telzrow CL, Campuzano A, Nichols CB, Munro C, Wormley FL, Jr, Alspaugh JA. 2018. Defects in intracellular trafficking of fungal cell wall synthases lead to aberrant host immune recognition. PLoS Pathog 14:e1007126. https://doi.org/10.1371/journal.ppat.1007126.
33. Pianalto KM, Billmyre RB, Telzrow CL, Alspaugh JA. 2019. Roles for stress response and cell wall biosynthesis pathways in caspofungin tolerance in Cryptococcus neoformans. Genetics 213:213–227. https://doi.org/10.1534/genetics.119.302290.